Research Square

Preprints are preliminary reports that have not undergone peer review.
They should not be considered conclusive, used to inform clinical practice,
or referenced by the media as validated information.

Root disturbance effects of diverse halophytes on soil nutrient elements and salt ions in intertidal ecotone of the Yellow River Estuary wetland

Debin Sun
Ludong University
Bo Guan
Ludong University
Yunzhao Li
Ludong University
Junbao Yu (yu.junbao@foxmail.com)
Ludong University
Fanzhu Qu
Ludong University
Jisong Yang
Ludong University
Xuehong Wang
Ludong University
Xue Li
Ludong University
Di Zhou
Ludong University

Research Article

Keywords: Halophytes, Root disturbance effect, Soil nutrients and ions, Intertidal ecotone, the Yellow River Estuary wetland

Posted Date: December 25th, 2023

DOI: https://doi.org/10.21203/rs.3.rs-3699490/v1

License: This work is licensed under a Creative Commons Attribution 4.0 International License.
Read Full License

Abstract

Four representative halophytes of *Tamarix chinensis* (Tc), *Phragmites australis* (TPa), *Suaeda salsa* (Ss) and *Spartina alterniflora* (Sa) in the Yellow River Estuary wetland were selected to clarify the root disturbance effects on soil nutrient elements, salt ions and their stoichiometric ratios. The results showed that the average TOC content of Tc, TPa, Ss, and Sa in the rhizosphere (RS) group were 5.19, 2.15, 2.05, and 2.14 times of those in the non-rhizosphere (CK) group, respectively. TN content of Tc in the RS group was about 3.44 times of the CK group. The average soil pH and salinity reduced by 3.60% and 41.35%, respectively, due to the root disturbance of Tc. Soil ions including K^+, Ca^{2+}, Mg^{2+}, Na^+, Cl^- and SO_4^{2-} reduced by 33.86%-62.86%. The root disturbance of TPa reduced soil pH and salinity by 1.09% and 35.47%, respectively, and soil ions reduced by 16.93%-46.85%. However, the root disturbance effects in Sa and Ss were not obvious. The results of Mantel test and PCA demonstrated that the root disturbance diversified the soil characteristics. The disturbance of roots played a crustal role in affecting the spatial heterogeneity of soil properties in the coastal wetlands above the intertidal zone (Tc and TPa), and its effect was greatly weakened below the intertidal zone (Sa and Ss). These findings are important for understanding how halophytes can impact soil nutrient levels and salt concentrations in coastal wetlands, which is crucial for effective management and restoration efforts.

1 Introduction

Soil plays a crucial role in regulating material conversion and energy flow in wetlands, thereby maintaining the ecosystem's internal stability (Yu et al., 2016). As a unique ecotone between terrestrial and marine ecosystems, the coastal wetland is an intensely dynamic, intricate and fragile system that provides vital ecological functions and services (Cao et al., 2015; Du et al., 2022). Soil properties exhibit typically spatial heterogeneity in many ecosystems. Low nutrient content and high salinity are two major characteristics of coastal wetland soil, leading to a high vulnerability of the ecosystem (Jia et al., 2017; Li et al., 2021b). As the primary soil nutrient elements, carbon (C), nitrogen (N), and phosphorus (P) are the basis for the composition of all living substances in the ecosystem (Qu et al., 2014; Meng et al., 2021). C constitutes the fundamental structure of plants and accounts for their biomass far beyond 50% (Xu et al., 2019). N is the basic component of enzymes and plays a pivotal role in photosynthesis and biological production (Rong et al., 2016). P is an essential element for nucleic acids and cell membranes and responsible for the composition of cellular structural DNA and RNA (Liang et al., 2020; Li et al., 2021a). The balance between energy and nutrients is known as ecological stoichiometry, which reflects the organisms' demand for natural resources. It predominantly connects biogeochemical cycles of soil C, N, and P at different levels (Xu et al., 2019; Muhammad et al., 2020). The soil C:N:P ratio reflects the nutrient balance and serves as an indicator of the coastal ecosystem's nutritional status (Qu et al., 2014; Li et al., 2021a). Soil salinity is a major abiotic stress affecting the physicochemical properties of soil. The high salinity stress leads to a decrease in soil quality, habitat conditions and biodiversity, which further restricts the stable development of coastal wetland ecosystems (Liu et al., 2017a; Wang et al., 2018). Soil salinification is characterized by an excessive concentration of soluble salt ions in soil solution (Zhu et

al., 1983). This directly affects the growth and development of plants, resulting in osmotic stress and ion toxicity, which in turn leads to the loss of biodiversity (Yi et al., 2007b; Jia et al., 2017; Zhao et al., 2022b). The spatial distribution characteristics of soil salinity have become a vital ecological factor influencing the distribution pattern of vegetation, plant-soil relationship, and productivity in coastal regions (Liu et al., 2018; Sun et al., 2022b; Zhao et al., 2022b).

The variation and distribution of nutrients and salt ions in coastal soil are influenced by various factors, such as climatic characteristics, hydrological processes, biological disturbances, and human activities (Yu et al., 2016, Liu et al., 2018; Sun et al., 2022b). The bioturbation, which is defined as the biological reworking of soils and sediments, has been regarded as an important component for soil processes and geomorphology (Meysman et al., 2006). Halophytes can survive in harsh environments, such as shallow groundwater tables, scarce freshwater, and insufficient nutrients. They distribute widely in coastal wetlands and become an important component of the coastal ecosystem (Jia et al., 2017; Jing et al., 2018; Li et al., 2021a). Coastal halophytes have developed varying degrees of saline tolerance due to long-term exposure to salinity stress, influenced by tidal action and soil evapotranspiration (María et al., 2004; Zhao et al., 2022b). Therefore, coastal halophytes commonly demonstrate a regular ribbon distinction from land to sea along different degrees of soil salinity (Sun et al., 2022b). Simultaneously, the soil properties are significantly impacted by the growth, development, and metabolism of halophytes, showing the dominant bioturbation in the coastal region (Yuan et al., 2016; Liu et al., 2017a; Wang et al., 2019). As the vital organ for obtaining soil nutrients, roots have a direct effect on soil properties through vigorous metabolism and complicated secretions (Liu et al., 2018). Thus, a close relationship between plants and soil in the rhizosphere was found (Jing et al., 2018; Wendel et al., 2022). Studies have found that halophytes have different rhizosphere effects under different conditions of soil salt, pH, soil texture, and nutrients (Yamamoto et al., 2018). Plants can alter soil physicochemical properties by releasing root exudates, shaping rhizosphere microbial communities (Yi et al., 2007a). Meanwhile, the rhizosphere possesses a radiative effect on the surrounding soil (Zhao et al., 2022a). Different plants have unique metabolic processes that lead to the production of distinct root exudates. Several studies revealed that around 11% of the net fixed C was exuded to the rhizosphere through roots, and these exudates also contain large amounts of N and P (Bais et al. 2006; Jones et al. 2009; Nakayama and Tateno 2018). Each halophyte can cause soil property differences between rhizosphere and bulk soils (Zhao et al., 2022c; Amir and Moshe et al., 2017). Yamamoto et al. (2018) studied soil microenvironment in the rhizosphere, root inner layer, and blank soil of two halophytes (*Glaux maritima* and *Salicornia europaea*) in saline-alkali land and found that soil nutrient elements and functional characteristics of different plant types were considerably different (Yamamoto et al., 2018). Jing et al. (2018) demonstrated that *Atriplex triangularis* and *Suaeda glauca* changed the rhizosphere soil properties and bacterial community significantly within 3 months planting (Jing et al., 2018). Additionally, a study by Tian et al. (2020) on rhizosphere in salinized soil at North Yinchuan revealed that *Medicago sativa* and *Achnatherum splendens* could modify the holistic soil conditions and enzyme activity (Tian et al., 2020). These studies reflect that the rhizosphere possesses important ecological functions for the interaction of soil and plants by root activities.

As a typical coastal wetland along the Pacific Coast, the Yellow River Estuary wetland covers a large area of salt marsh in the intertidal zone (Yu et al., 2016). The predominant halophytes include *Tamarix chinensis*, *Phragmites australis* (tidal salt community), *Suaeda salsa* and *Spartina alterniflora* in the natural coastal wetland of the Yellow River Estuary (Liu et al., 2018; Zhao et al., 2022c). Most community structure is simple and dominated by one plant species with few concomitants. Under the function of land-sea-river interaction, the dominant vegetation is distributed with a zonal sequence from land to sea. The ecological ecotone between terrestrial and marine ecosystems has become a vital region for biogeochemical processes in the estuary (Li et al., 2021b; Sun et al., 2022b). Affected by poor soil nutrition and high salinity, the ecotone ecosystem is fragile. Halophytes play a key role in facilitating material circulation, resisting salt accumulation, maintaining biodiversity and protecting the steady infrastructure in the coastal zone (María et al., 2010; Yuan et al., 2016; Zhao et al., 2022c). For the Yellow River Estuary wetland, the adaptation mechanism of *Suaeda salsa* to low nitrogen habitat and its soil improvement effect on coastal heavy saline-alkaline soil were investigated by several previous studies (Liu et al., 2017b; Yang et al., 2019). The results showed that the intertidal population seedlings had a higher capability for NO_3^--N reutilization to maintain nitrogen metabolism and normal photosynthesis. The *Suaeda salsa* has an obvious effect on reducing soil salinity in coastal regions. Besides, under tidal and short-term flooding conditions, the mass losses of *Phragmites australis* litter were 25.21% and 19.22%, respectively, during the experimental period. Under the identical above conditions, the mass losses of *Suaeda salsa* litter were 37.08% and 28.49%, respectively (Guan et al., 2020). The investigations of the salt characteristics, homeostasis characteristics and intrinsic relationships in the plant-soil system found that the total carbon, total nitrogen, and N: P values of the halophyte communities in the surface soil (0–20 cm) were significantly higher than the other layers because of root activity (Zhao et al., 2022b). However, few references about the rhizosphere bio-disturbance effects of diverse halophytes along the intertidal ecotone in the Yellow River Estuary wetland have been caught. Therefore, based on the field measurement results of soil properties in the rhizosphere and non-rhizosphere, the soil feature changes by halophyte root disturbance in the Yellow River Estuary wetland were explored. The objectives of the study are to (1) investigate the contents of soil C, N, P and salt ions of different halophyte types in rhizosphere and non-rhizosphere, (2) compare the effects of root disturbance on soil properties under different halophytes, and (3) reveal the dominant factors for soil synthetical property characteristics change in the ecological ecotone of the Yellow River Estuary.

2 Materials and methods

2.1 Study area

This study was conducted in the Yellow River Estuary wetland (37°42'0"-37°51'0"N, 119°7'30"-119°15'0"E) (Fig. 1). The study area is a warm-temperate and continental monsoon climate with distinct seasons. The average annual temperature, precipitation, and evaporation are 12.8℃, 537.3 mm, and 1,928.2 mm, respectively (He and Cui, 2015). The precipitation mainly concentrates in summer and autumn. The main freshwater supplement is atmospheric precipitation and rivers. *Tamarix chinensis*, *Phragmites australis*,

and *Suaeda salsa* are predominant native plant communities, and the *Spartina alterniflora* is an invasive species. Both of the four halophytes are widely distributed in the intertidal zone of the Yellow River Estuary. Due to the interactive effects of land and sea, the communities of *Tamarix chinensis*, *Phragmites australis*, *Suaeda salsa* and *Spartina alterniflora* show a regular ribbon distribution from land to sea (Sun et al., 2022b). The predominantly soil types are swampy soil and saline soil (Yu et al., 2016).

2.2 Sample collection and measurement

The *Tamarix chinensis* (Tc), *Phragmites australis* (tidal salt community, TPa), *Suaeda salsa* (Ss) and *Spartina alterniflora* (Sa) were selected as study objects. Soil samples of rhizosphere and non-rhizosphere from Tc, TPa, Ss and Sa were collected at low tide in September 2020 (Fig. 1). Six parallel sample sites were set up at each typical community and three duplicate soil samples were collected at each site (Fig. 1). The soil of non-rhizosphere (CK group, 0–10 cm) was collected by core sampler sterile spatulas. The soil at halophyte rhizosphere (RS group, 0–10 cm) was collected by the shaking root method. Three duplicate soil samples were collected and mixed homogeneity *in situ* after removing plant residues, roots, and debris. Then the air-dried soil samples were sieved with a 0.149-mm diameter nylon sieve after grinding by a mortar to determine soil properties.

Soil total organic carbon (TOC) was determined by TOC Analyzer (vario TOC cube, Elementar, Germany) after inorganic carbon was eliminated using 1M HCl. Soil total nitrogen (TN) and total phosphorus (TP) were determined by a continuous flow analyzer (Futura A16786, Alliance, France) after digestion and filtration. Soil NH_4^+-N and NO_3^--N in supernatant liquor were filtrated by a 0.45-μm membrane after extraction with 2 M KCl from sieved dry soil samples; and then were determined by a continuous flow analyzer. After extraction and dilution, the concentration of soil K^+, Na^+, Ca^{2+}, Mg^{2+}, Cl^-, and SO_4^{2-} were measured by Ion Chromatography (Dionex ICS3000, DIONEX, America). Soil pH (water: soil = 2.5:1) and salinity (water: soil = 5:1) were determined by a pH meter (FE28-Standard, Mettler Toledo, Switzerland) and an electrical conductivity meter (FE38, Mettler Toledo, Switzerland), respectively. Soil particle size and mean soil particle size (MPS) were measured by a laser particle size analyzer (Mastersizer 2000, Malvern Panalytical, United Kingdom). The stoichiometric ratios of C/N, C/P and N/P were calculated by the amount of TOC, TN, and TP ($mol \cdot kg^{-1}$). The soil sodium-adsorption ratio (SAR), Cl^-/SO_4^{2-}, $(Na^+ + K^+)/(Ca^{2+} + Mg^{2+})$, and Mg^{2+}/Ca^{2+} were calculated by the amount of soil salt ions ($mol \cdot kg^{-1}$) (Chi et al., 2011). The formula for the enrichment ratio (E) of each soil property of the rhizosphere was referred to Du (Du et al., 2011).

2.3 Data analysis

The data on soil properties were normalized and scaled to statistical analysis. Differences among soil types were tested using analysis of variance (ANOVA) with a post hoc test (Tukey test) in the software Statistical Product and Service Solutions (SPSS v.24.0). A *p*-value less than 0.05 denoted statistical significance. The relationships of soil properties were determined by Pearson's correlation analysis

method in R v4.2.3. Mantel test and Principal Component Analysis (PCA) were run in R v4.2.3. Software of Origin 9.1 was used to draw data figures.

3 Results

3.1 Soil pH, Sa and MPS of rhizosphere in different halophyte types

The mean values of soil pH in different types were between 8.29–8.71 (Fig. 2A). The pH values of Ss were the highest than other types both in CK group and RS group. A significant difference in pH values between CK group and RS group was observed in Tc and TPa ($p < 0.05$). The mean values of soil salinity in different types were between 0.85–1.79 (Fig. 2B). The soil salinity values of CK group showed that the values of TPa were significantly higher than Ss and Sa group ($p < 0.05$). In RS group, the soil salinity of TPa was higher than Tc ($p < 0.05$). There were significant differences in soil salinity between CK group and RS group in Tc and TPa ($p < 0.05$). The variation trend of mean soil particle size of CK group and RS group in different halophyte types followed as Tc > Sa > Ss > TPa (Fig. 2C). For soil particle proportion, the silt proportion in the study area reached more than 50% in each soil type and was significantly higher than clay and sand ($p < 0.05$) (Fig. 2D). The clay proportion of TPa were obviously higher than that of others ($p < 0.05$). The sand particle proportion of Tc in RS group was lower than that of CK group ($p < 0.05$).

3.2 Soil C, N, P and ecological stoichiometry of rhizosphere in different halophyte types

There were significant differences in TOC content among four halophyte types ($p < 0.05$) (Fig. 3A). The TOC contents of the RS group were significantly higher than that of the CK group in each halophyte types ($p < 0.05$). TOC contents of TPa and Sa were higher than that of Tc ($p < 0.05$) in both the CK group and RS group ($p < 0.05$). The TN content of TPa was higher than that of Sa and Tc in the CK group ($p < 0.05$), while the TN content of Tc in the RS group was higher than that of others ($p < 0.05$) (Fig. 3B). The TN contents of Tc in RS group were higher than that of CK group ($p < 0.05$). There was no significant difference in TP content in CK group among the four types ($p > 0.05$) (Fig. 3C). In Tc, the TP contents of the RS group were higher than that of the CK group ($p < 0.05$). According to the confidence distribution of TOC, TN and TP, the confidence intervals of TOC (Fig. 3D) and TN (Fig. 3E) in rhizosphere soil were of obvious differences, while TP (Fig. 3F) were relatively stable. The C/P values followed as TPa > Ss > Tc in the CK group and TPa > Sa > Ss in the RS group ($p < 0.05$) (Fig. 3G). The C/P values in each halophyte type of the RS group were higher than those of the CK group ($p < 0.05$). The maximum mean C/P values were observed in TPa in both two groups. The C/N values of four halophyte types in the RS group were higher than those in the CK group ($p < 0.05$) (Fig. 3H). The C/N values of TPa, Ss and Sa were higher than that of Tc in both the CK group and the RS group ($p < 0.05$). The N/P values showed an order of TPa > Ss and Tc in CK group and an order of Tc > TPa > Sa and Ss in RS group ($p < 0.05$) (Fig. 3I). In Tc, the N/P

values of the RS group were considerably higher than that of CK group ($p < 0.05$). The comprehensive difference of soil C, N and P resulted in significant spatial heterogeneity of soil ecological stoichiometry in the rhizosphere which was caused by root disturbance (Fig. 3J).

3.3 Soil salt ions contents of the rhizosphere in different halophyte types

The values of soil K^+, Ca^{2+}, Mg^{2+} and Na^+ in different halophyte types ranged 0.11–0.26 g·kg^{-1}, 0.13–0.29 g·kg^{-1}, 0.15–0.49 g·kg^{-1}, and 4.07–6.50 g·kg^{-1} (Fig. 4A), respectively. The highest and lowest contents of K^+ were observed in Sa and Tc of the RS group, respectively. There were significant differences of K^+ contents of Tc, TPa, and Ss between the CK and RS groups ($p < 0.05$). The highest and lowest contents of Ca^{2+} and Mg^{2+} were observed in Tc of the CK group and Ss of the RS group. The highest and lowest contents of Na^+ were observed in TPa of the CK group and Tc of the RS group. The contents of K^+, Ca^{2+}, Mg^{2+} and Na^+ of Tc and TPa in CK group were higher than those in the RS group ($p < 0.05$). The values of soil NO_3^--N, SO_4^{2-}, NH_4^+-N, and Cl^- in different types ranged 0.92–5.82 mg·kg^{-1}, 1.22–2.01 g·kg^{-1}, 1.85–6.79 mg·kg^{-1}, and 4.41–10.69 g·kg^{-1} (Fig. 4B), respectively. The highest values of NO_3^--N and NH_4^+-N were observed in Tc of the RS group and TPa of RS group, respectively, while the values of both SO_4^{2-} and Cl^- appeared in TPa of the CK group. The lowest contents of NO_3^--N, SO_4^{2-}, NH_4^+-N and Cl^- were found in TPa of the CK group, Ss of the RS group, Ss of the CK group and Tc of the RS group, respectively. There were significant differences of NO_3^--N, SO_4^{2-}, NH_4^+-N and Cl^- in Tc and TPa between CK and RS groups ($p < 0.05$). The contents of NO_3^--N and NH_4^+-N of Tc and TPa in the RS group were higher than those in the CK group, while the contents of SO_4^{2-} and Cl^- were contrary. Compared with CK, the soil Cl^- contents of Tc and TPa in the RS group decreased by 58.44% and 33.21%, respectively. Only the contents of NH_4^+-N and NO_3^--N in studied ions of Tc and TPa in the RS group were higher than those in the CK group, indicating that the plant root plays an important role in soil salinity improvement because both of them are available nutrients.

The CV values of soil ions in four halophyte types showed an obviously regular change (Fig. 4C). Between the CK group and RS group, the CV values of Mg^{2+} and NO_3^--N were higher than that of others in each type, reflecting a high spatial variability for Mg^{2+} and NO_3^- appeared in the study area under the influence of root disturbance. The CV values of soil ions in Tc and TPa were considerably higher than those in Ss and Sa, indicating that the root disturbance for soil major salt ions of Tc and TPa was considerably higher than that of Ss and Sa.

The value ranges of soil sodium-adsorption ratio (SAR), Cl^-/SO_4^{2-}, DIN/TN, $(Na^+ + K^+)/(Ca^{2+} + Mg^{2+})$ and Mg^{2+}/Ca^{2+} in different types were between 52.75–95.55, 9.55-18.00, 1.93%-3.78%, 9.50-19.94, and 1.57–2.77, respectively (Fig. 5A-E). There were significant differences of SAR, Cl^-/SO_4^{2-}, DIN/TN and Mg^{2+}/Ca^{2+} in Tc and TPa between CK and RS group ($p < 0.05$) and those values of SAR, Cl^-/SO_4^{2-},

Mg^{2+}/Ca^{2+} of Tc and TPa in CK group were higher than those in RS group, while the results were reversed for DIN/TN of Tc and TPa. There was no significant difference for DIN/TN among the four types in the CK group ($p > 0.05$). The CV values of soil SAR, Cl^-/SO_4^{2-}, DIN/TN, and Mg^{2+}/Ca^{2+} in each halophyte type showed a regular change (Fig. 5F). The CV value of DIN/TN of each type in both the CK group and RS group was the largest. The CV values of soil DIN/TN, SAR, Cl^-/SO_4^{2-}, and Mg^{2+}/Ca^{2+} of four halophytes followed as Tc > TPa and Sa > Ss. The order indicated that the above four indexes had the maximum spatial changes with and without root disturbance in Tc and had the minimum spatial changes in Ss.

3.4 The analysis of soil properties

The correlation analysis results of the CK group showed that there was an intensively positive correlation among TOC, TN, TP, and among K^+, Ca^{2+}, Mg^{2+}, Na^+, Cl^- and SO_4^{2-}, respectively ($p < 0.05$) (Fig. 6A). Soil salinity was positively correlated with metal cations, Cl^- and SO_4^{2-} ($p < 0.05$) and negatively correlated with soil silt, sand, and MPS. Soil clay was positively correlated with C, N, P, and K, and negatively correlated with NO_3^-. The correlations between sand proportion with others were completely opposite to soil clay. The correlation analysis results of the RS group showed that positive correlations existed in K^+ with Mg^{2+}, Na^+, NH_4^+, NO_3^-, pH, salinity and clay proportion, while the opposite correlations were observed in SO_4^{2-} with others ($p < 0.05$) (Fig. 6B). The significant correlations of SAR and Cl^-/SO_4^{2-} with TOC, TN, TP was not observed. The correlation between SAR and Cl^-/SO_4^{2-} was positive ($p < 0.05$). pH was negatively correlated with TN, TP, SO_4^{2-}, silt proportion, sand proportion, and MPS ($p < 0.05$), and positively correlated with K^+, Na^+, NH_4^+, salinity and soil clay proportion ($p < 0.05$). The clay proportion was negatively correlated with TN, TP, and SO_4^{2-}, and the silt proportion was negatively correlated with TOC, K^+, Mg^{2+}, Na^+, Cl^-, NH_4^+, NO_3^-, pH, and salinity ($p < 0.05$). Compared to the CK group, the positive correlations among C, N, P and K in the RS group were decreased, and this change was also observed between salt ions (i.e. Ca^{2+}, Mg^{2+}, Na^+, Cl^-, SO_4^{2-}, and NH_4^+).

The principal component analysis (PCA) was selected to analyze the response of soil nutrient elements, soil salt ions, and soil texture to root disturbance in different halophyte types (Fig. 7A-C). The cumulative interpretation degree of the first two principal components to the overall data characteristics reached 58.3% (Fig. 7A). The obvious differences between the CK group and RS group of the point distribution and confidence ellipse appeared in Tc and TPa. On the contrary, the point distribution of the CK group and RS group in Ss and Sa is relatively concentrated. The PCA results showed that the root disturbance effects on soil comprehensive properties in Tc and TPa were much stronger than those in Ss and Sa. In the CK group, axes 1 and axes 2 could explain 45.2% and 30.7% characteristics of the overall data (Fig. 7B), respectively. The main indicators were soil sand proportion, MPS, and NO_3^--N, corresponding to soil TOC, C/P, TN, N/P, SAR and clay proportion. In the RS group, axes 1 and axes 2 could explain 43.2% and 20.8% characteristics of the overall data (Fig. 7C), respectively. The main influence indicators at axes 1 direction were soil silt proportion, TP, NO_3^--N, and pH and those were soil Ca^+, and NH_4^+-N at axes 2

direction. The scree plot analysis results showed that there were two dominant components in the CK group and three dominant components in the RS group (Fig. 7B-C), suggesting that the soil property characteristics tended to be diversified under the influence of root disturbance, which was consistent with the results of correlation analysis (Fig. 6). The mantel test showed that the soil C, N, and P matrices significantly correlated with the soil saline-alkali characteristics and soil texture ($r > 0.2$, $p < 0.05$), and significantly influenced by root disturbance in TC and TPa ($r > 0.2$, $p < 0.05$) (Fig. 7D). The correlation degree in Ss and Sa were significantly reduced, which was consistent with the results of PCA results.

4 Discussion

4.1 The root disturbance effects of soil nutrient elements in halophytes rhizosphere in the Yellow River Estuary

As the dominating bio-disturbance in coastal wetlands, roots of halophytes played a critical role in the processes of nutrient element transformation. A previous study confirmed that the rhizosphere had a great cementing effect on TOC (Batista et al., 2022). Global patterns of rhizosphere effects on soil carbon biogeochemical processes showed that rhizosphere effects could significantly enhance the soil carbon cycle (Ma et al., 2023). Consistent with previous studies, our results showed that the average TOC content of Tc, TPa, Ss, and Sa in RS group were 5.19, 2.15, 2.05, and 2.14 times of those in CK group, respectively (Fig. 3A). The rhizosphere effects for soil carbon accumulation were mainly caused by the decomposition of root litter and the organic acids secreted by plant roots (Gan et al., 2021; Zhao et al., 2022a). These rhizosphere effects were higher in humid regions than in arid regions and higher in wetlands covered by woody plants than in herbaceous plants (Wang et al., 2021; Ma et al., 2023). The TOC content in the rhizosphere of Tc reached 5.19 times than in non-rhizosphere ($p < 0.05$) and much higher than others ($p < 0.05$) (Fig. 3A). The main reason was that the underground biomass of Tc and its disturbance intensity to the soil was much higher than those of others (Mahbobeh et al., 2019; Sun et al., 2022a). Besides, changes in tidal action and the drying-rewetting cycle can enhance the pathway of carbon loss in a tidal zone (Li et al., 2020). The results indicated that the halophyte root was beneficial to soil carbon accumulation, especially Tc in the study area.

In the Tc rhizosphere, the changes of TOC and TN in soil were considerably synergistic, which was consistent with the study of the “fertile island effect” (Cao et al., 2021; Gao et al., 2022). However, the significant difference in TN between CK and RS groups was only observed in Tc ($p < 0.05$). TN content of Tc in the RS group was about 3.44 times of the CK group (Fig. 3B). This might be explained that the Tc community was located at a high tidal flat and small proportion of N loss by the tide. In addition, the high biomass and litter amount of Tc caused a strong effect on soil carbon and nitrogen enrichment, leading to the significant “fertile island effect” of the rhizosphere appeared. The cooperativity of TOC and TN was not observed in the rhizosphere of TPa, Ss and Sa, mainly resulting in soil nitrogen loss due to tidal erosion. The sampling sites of TPa, Sa, and Ss located at the intertidal zone where the proportion of silt was high (more than 50%) (Fig. 2D). The soil erosion was easily occurred by the frequent tide (Fig. 1), leading to a lot of soil nitrogen loss (Zheng et al., 2020; Zhang et al., 2022). Furthermore, in the

alternating oxidation-reduction environment, the intensity of soil nitrogen loss by tidal rewetting triggers pulses was much greater than that of carbon (Emery et al., 2021; Zhang et al., 2022).

There was no significant difference in soil TP contents among studied soil types ($p > 0.05$) in both the CK group and RS group (Fig. 3C). The soil TP in the study area was mainly constituted by inorganic phosphorus (> 85%) which was principally imported by the Yellow River (Qu et al., 2018; Liang et al., 2020). The source of sediment and the saline-alkali environment of coastal wetland jointly determine the relatively stable content of soil TP in the study area (0.5–0.7 $g \cdot kg^{-1}$) (Meng et al., 2021). Therefore, root disturbance from halophytes for soil TP was extremely small in newborn wetlands (Yu et al., 2016; Qu et al., 2021).

4.2 The root disturbance effects on soil ecological stoichiometry in halophytes rhizosphere in the Yellow River Estuary

As a sensitive index to manifest soil environment change, C/N can reflect the circulation of soil organic carbon and nitrogen (Huang et al., 2021), C/P can be used to indicate the mineralization capacity of soil organic phosphorus (Wang et al., 2019)d can reflect the supply capacity and limiting level of soil nutrients (Muhammad et al., 2020). We observed that the C/N values and C/P values in the RS group were obviously higher than those in the CK group (Fig. 3H; Fig. 3G). The average C/N values in CK and RS groups were 19.12 and 39.23, respectively ($p < 0.05$), and the C/P values were 17.10 and 42.41, respectively ($p < 0.05$). The high C/N values of the RS group illustrated that halophyte roots could create a soil environment that could be conducive to the continuous accumulation of organic matter (Xiong et al., 2022). To support our results, Du (Du et al., 2022) found that the C/N/P of each sampling site was high in the surface soils with plant root disturbance and decreased with depth based on ^{137}Cs dating technology in the study area. The values of the CK group were much lower than the optimal C/N value (25) for soil organic matter decomposition (Ye et al., 2018; Elizabeth et al., 2020), because the decomposition of soil organic matter was quick and the nutrient accumulation was low in the intertidal zone (Xu et al., 2019; Meng et al., 2021). The average N/P values in CK and RS groups were 0.88 and 1.24, respectively, and the obvious difference was only observed in Tc ($p < 0.05$) (Fig. 3I). The N/P and C/N/P were relatively low, indicating the Yellow River Delta intertidal wetland was a N-limited ecosystem (Cao et al., 2015; Qu et al., 2017; Sun et al., 2022b). As an essential nutrient element for plant growth and development, nitrogen is an important limiting element that affects the primary productivity of coastal wetland ecosystems (Cheng et al., 2020; Sun et al., 2022). The significant difference in N/P values of Tc between the CK group (0.64) and RS group (2.00) suggested that the rhizosphere of Tc could promote the transformation rate of nitrogen and reduce the nitrogen limitation in the ecosystem. The NH_4^+-N and NO_3^--N contents of Tc in RS group was 1.49 times and 2.43 times than that in CK group ($p < 0.05$), respectively (Fig. 4B), and the CV of NH_4^+-N (34.32) and NO_3^--N (53.34) of Tc were obviously higher than that in Ss and Sa (Fig. 4C), which could verify the results of eco-stoichiometry. The significant differences in N/P values of TPa, Ss and Sa between the CK group and RS group were not observed, because the soil N loss and relatively stable content of soil TP as mentioned above.

4.3 The root disturbance effects on soil saline-alkali characteristics in halophytes rhizosphere in the Yellow River Estuary

Soil pH, salinity, salt ions content, as well as salt ion stoichiometric ratios are important indicators to characterize soil saline-alkali property and soil salt type (Wang et al., 2018; Hartemink et al., 2023). Compared with CK group, the average pH of Tc and TPa in RS group decreased by 3.60% and 1.09% ($p < 0.05$), respectively (Fig. 2A), and the average salinity decreased by 41.35% and 35.47% ($p < 0.05$), respectively (Fig. 2B). Several studies related soil salt ions and homeostasis characteristics of halophytes showed that the strategies for salt tolerance were the critical factors affecting the relationship between plants and soil environments (Maria et al., 2004; Li et al., 2021b; Lau et al., 2012). *Phragmites australis* and *Suaeda salsa* tend to form similar rhizosphere soil environments in the intertidal zone to cope with high salt stress through physiological metabolism and root exudates (Li et al., 2021a; Zhao et al., 2022c). Therefore, the resistance and recovery ability of rhizosphere soil were higher than that of bulk soils (Yuan et al., 2016; Yamamoto et al., 2018).

The significant differences of K^+, Ca^{2+}, Mg^{2+}, Na^+, Cl^-, and SO_4^{2-} between CK and RS groups were observed in Tc and TPa ($p < 0.05$) (Fig. 4A-B). The Tc had a strong absorption effect on soil nutrient elements and salt ions by root. Tc acts as “salt pumps” to transfer salt ions out of the soil system (Sun et al., 2022a). Under a high salinity environment, TPa roots had a selective absorption ability for salt ions (Li et al., 2021b). When plants grow vigorously, the rate of ion migration to the root surface is slower than root absorption, causing an ion deficit in the rhizosphere (Yi et al., 2007a; Ge et al., 2018). In addition, a “preferential path” formed by the exuberant transverse brat roots of TPa in 0–20 cm depth reduced the surface accumulation ability of the rhizosphere soil environment (Li et al., 2021b). The chloride migrates more actively than sulfate in the ascending process of salt ions (Andreas et al., 2001; Dong et al., 2013), resulting in much greater spatial variability of Cl^- in Tc and TPa than that of SO_4^{2-} (Fig. 4C). Compared with the bulk soil with intense salt accumulation, the salt ions content decreased significantly in the rhizosphere. However, the significant difference in ion contents between the CK and RS groups did not exist in Ss and Sa ($p > 0.05$) (Fig. 4). The dominant reason is that the tidal action strongly interfered with the spatial distribution of salt ions in the rhizosphere soil at intertidal ecotone zone. Based on the salt ion stoichiometry, the soil salinity composition types of the study area were mainly sodium chloride salt and magnesium sulfate-sodium chloride salt (Zhu et al., 1983; Wang et al., 1993). The soil SAR in the study area was much higher than 13, and the soil salinity was higher than the critical threshold value of saline-soil grade (0.6%). Therefore, the soil in the study area belongs to saline-alkali soil and the soil salinization degree is serious (Jia et al., 2017; Wang et al., 2018). Due to the SAR value is determined by Na^+, Mg^{2+} and Ca^{2+} contents, the migration rate of Na^+ in soil was higher than that of Mg^{2+} and Ca^{2+} under the condition of repeated flooding (Hasegawa et al., 2000). Our results showed that the values of SAR, Cl^-/SO_4^{2-}, Mg^{2+}/Ca^{2+} of Tc and TPa in CK group were higher than those in RS group, while the results were reversed for DIN/TN of Tc and TPa (Fig. 5). The change of salt ions in rhizosphere soil might be caused by the selective absorption and different absorption rates of ions by the root system (Yi et al., 2007a). The calcium salt is easy to fix in the condition of high pH in the CK group, while sodium salt

exists in soil solution with a free state (Zhao et al., 2022b). Plant root activities can provide sufficient Ca^{2+} to replace Na^{+} (Qadir et al., 2001; Li et al., 2021a), leading to the CV of Na^{+} is much lower than that of Ca^{2+}. Therefore, In Tc and TPa rhizosphere, the significant differences of soil SAR, pH, soil salinity and salt ions to the CK group suggested that the root disturbance of Tc and TPa could reduce the relative activity of sodium-soil exchange reaction and the soil alkalinity. However, the tidal effect on the region of Ss and Sa located below the intertidal zone caused the homogenization of soil properties. The PCA and mantel test results (Fig. 7) also can support the above opinions about the root disturbance effects on soil comprehensive properties of studied soil types.

5 Conclusions

In this study, the root disturbance effects of four representative coastal halophytes on soil nutrient elements, salt ions and their stoichiometric ratios were evaluated in the Yellow River Estuary. The results demonstrated that the strong effects of root disturbance occurred in Tc and Tpa. The obvious “fertile island effect” appeared in the rhizosphere of Tc and Tpa, which had the high mitigation capability to soil nitrogen limitation. However, the effects of root disturbance of Ss and Sa were not obvious. The differences in soil pH, soil salinity and salt ions in Tc and TPa between CK and RS groups were synergistic. An obvious “salt valley effect” appeared in the Tc and TPa rhizosphere, which could assist the soil desalting. The root disturbance of Tc and TPa located above the intertidal zone performed a vital factor affecting the spatial heterogeneity of soil properties. However, the root disturbance of Sa and Ss located below the intertidal zone was weakened greatly because of the tidal effect, leading to the homogenization of soil properties. Our results illustrated that the effects of halophyte root disturbance on soil nutrient elements of the rhizosphere in coastal wetlands depended to a large extent on the tidal situation.

Declarations

Acknowledgements We thank Mr. Zhicheng Qu for the contribution to the field work.

Author Contributions The field work was performed by D. Sun, B. Guan, Y. Li, F. Qu, J. Yang, X. Wang, X. Li, and D. Zhou. Data analysis and interpretation were performed by D. Sun. The work was supervised by J. Yu. The first draft of the manuscript was written by D. Sun. All the authors read and approved the final manuscript.

Funding This work was supported by the National Natural Science Foundation of China (Grant numbers U1806218 and U2006215) and the National Key R&D Program of China (Grant number 2017YFC0505902).

Data Availability The datasets generated during and/or analysed during the current study are available from the corresponding author on reasonable request.

Competing Interests The authors have no relevant financial or non-financial interests to disclose.

References

1. Amir N, Moshe A. The functioning of rhizosphere biota in wetlands - a review[J]. Wetlands, 2017, 37(4): 615-633. DOI: 10.1007/s13157-016-0757-4.
2. An Y, Gao Y, Liu X, et al. Soil organic carbon and nitrogen variations with vegetation succession in passively restored freshwater wetlands[J]. Wetlands, 2021, 41(1): 1-10. DOI: 10.1007/S13157-021-01413-W.
3. Andreas R, Dan B. Nutritional interactions in mixed species forests: a synthesis[J]. Canadian Journal of Forest Research, 2001, 31(11): 1855-1870. DOI: 10.1139/x01-120.
4. Batista A, Libardi P, Alves M, et al. Electrochemical effects on clay dispersion in rhizo- and non-rhizospheric soils[J]. Journal of Soil Science and Plant Nutrition, 2022, 22(3): 3518-3526. DOI: 10.1007/S42729-022-00906-9.
5. Cao L, Song J, Li X, et al. Geochemical characteristics of soil C, N, P, and their stoichiometrical significance in the coastal wetlands of Laizhou Bay, Bohai Sea[J]. CLEAN-Soil, Air, Water, 2015, 43(2): 260-270. DOI: 10.1002/clen.201300752.
6. Cao Y, Su Y, Huang G, et al. Soil texture modulates the intensity of fertile islands through affecting the distribution of shrub fine roots[J]. Journal of Arid Environments, 2021, 189(7): 104503. DOI: 10.1016/J.JARIDENV.2021.104503.
7. Cheng H, Jiang Z, Ma X, et al. Nitrogen dynamics in the mangrove sediments affected by crabs in the intertidal regions. Ecotoxicology, 2020, 29(6): 669-675. DOI: 10.1007/s10646-020-02212-5.
8. Chi C, Zhao C, Sun X, et al. Estimating exchangeable sodium percentage from sodium adsorption ratio of salt-affected soil in the Songnen plain of northeast China[J]. Pedosphere, 2011, 21(02): 271-276. DOI: 10.1016/S1002-0160(11)60127-6.
9. Dong H, Du Z, Ma B, et al. Dynamic changes of water and salt in soils of different plantations in the Yellow River Delta[J]. Journal of Soil and Water Conservation, 2013, 27(05): 48-53. DOI: 10.13870/j.cnki.stbcxb.2013.05.051.
10. Du M, Zhang L, Liang K, et al. Characteristics of nitrogen and organic carbon content in rhizosphere and bulk soil under different shrubs in the alpine sandy grassland[J]. Chinese Journal of Grassland, 2011, 33(04): 18-23.
11. Du S, Bai J, Zhao Q, et al. Deposition flux, stocks of C, N, P, S, and their ecological stoichiometry in coastal wetlands with three plant covers[J]. Frontiers in Ecology and Evolution, 2022: 199. DOI: 10.3389/FEVO.2022.840784.
12. Elizabeth C. C, Clive A. K, John A. K, et al. Microorganisms and nutrient stoichiometry as mediators of soil organic matter dynamics[J]. Nutrient Cycling in Agroecosystems, 2020, 117(3): 273-298. DOI: 10.1007/s10705-020-10076-8.
13. Emery H E., Angell J H., Tawade A, et al. Tidal rewetting in salt marshes triggers pulses of nitrous oxide emissions but slows carbon dioxide emission[J]. Soil Biology and Biochemistry, 2021, 156(5): 108197. DOI: 10.1016/J.SOILBIO.2021.108197.

14. Gan D, Feng J, Han M, et al. Rhizosphere effects of woody plants on soil biogeochemical processes: A meta-analysis[J]. Soil Biology and Biochemistry, 2021, 160: 109310. DOI: 10.1016/J.SOILBIO.2021.108310.
15. Gao Y, Tariq A, Zeng F, et al. “Fertile islands” beneath three desert vegetation on soil phosphorus fractions, enzymatic activities, and microbial biomass in the desert-oasis transition zone, Catena, 2022, 212: 106090. DOI: 10.1016/j.catena.2022.106090.
16. Ge L, Li J, Li L, et al. Effect of Phragmites communis on Salt Modification in Saline-alkaline Soil[J]. IOP Conference Series: Earth and Environmental Science, 2018, 170(3). DOI: 10.1088/1755-1315/170/3/032086.
17. Guan Y, Bai J, Wang W, et al. Litter decomposition and heavy metal return characteristics of *Phragmite australis* and *Suaeda salsa* under different flooding conditions in the Yellow River Delta, China[J]. Journal of Natural Resources, 2020, 35(02): 472-479. DOI: 10.31497/zrzyxb.20200218.
18. Hasegawa P M., Bressan R A., Zhu J, et al. Plant cellular and molecular responses to salinity[J]. Annual Review of Plant Physiology and Plant Molecular Biology, 2000, 51: 463-499. DOI: 10.1146/annurev.arplant.51.1.463.
19. Hartemink A E, Barrow N J. Soil pH-nutrient relationships: the diagram[J]. Plant and Soil, 2023(prepublish). DOI: 10.1007/s11104-022-05861-z.
20. He Q, Cui B. Multiple mechanisms sustain a plant-animal facilitation on a coastal ecotone. Scientific Reports, 2015, 5(1): 8612. DOI: 10.1038/srep08612.
21. Huang J, Yuan Z. Ecological stoichiometric characteristics of soil SOC, TN, and TP under different restoration methods in Qixing River wetland. Journal of King Saud University-Science, 2021, 33(4), 101407. DOI: 10.1016/J.JKSUS.2021.101407.
22. Jia J, Huang C, Bai J, Zhang G, et al. Effects of drought and salt stresses on growth characteristics of euhalophyte *Suaeda salsa* in coastal wetlands[J]. Physics and Chemistry of the Earth, 2017, 103: 68-74. DOI: 10.1016/j.pce.2017.01.002.
23. Jiang H, Ma J, Xu H, et al. Multiple isotopic compositions reveal complex nitrogen cycling in a subtropical estuary[J]. Environmental Pollution, 2020, 272: 116410. DOI: 10.1016/J.ENVPOL.2020.116410.
24. Jiang Y, Yin G, Li Y, et al. Saltwater incursion regulates N_2O emission pathways and potential nitrification and denitrification in intertidal wetland[J]. Biology and Fertility of Soils, 2022 (prepublish). DOI: 10.1007/S00374-022-01625-0.
25. Jing C, Xu Z, Zou P, et al. Coastal halophytes alter properties and microbial community structure of the saline soils in the Yellow River Delta, China[J]. Applied Soil Ecology, 2018, 134: 1-7. DOI: 10.1016/j.apsoil.2018.10.009.
26. Jones D L, Nguyen C, Finlay R D. Carbon flow in the rhizosphere: carbon trading at the soil-root interface[J]. Plant Soil, 2009, 321: 5-33. DOI: 10.1007/s11104-009-9925-0.
27. Lau J A, Lennon J T. Rapid responses of soil microorganisms improve plant fitness in novel environments[J]. Proceedings of the National Academy of Sciences of the United States of America,

2012, 109(35): 14058-14062. DOI: 10.1073/pnas.1202319109.

28. Li J, Qu W, Han G, et al. Effects of Drying-Rewetting Frequency on Vertical and Lateral Loss of Soil Organic Carbon in a Tidal Salt Marsh[J]. Wetlands. 2020, 40:1433-1443. DOI: 10.1007/s13157-020-01286-5.
29. Li T, Sun J, Fu Z. Halophytes differ in their adaptation to soil environment in the Yellow River Delta: effects of water source, soil depth, and nutrient stoichiometry[J]. Frontiers in Plant Science, 2021a, 12: 675921-675921. DOI: 10.3389/FPLS.2021.675921.
30. Li Y, Kang E, Song B, et al. Soil salinity and nutrients availability drive patterns in bacterial community and diversity along succession gradient in the Yellow River Delta[J]. Estuarine, Coastal and Shelf Science, 2021b, 262: 107621. DOI: 10.1016/J.ECSS.2021.107621.
31. Liang B, Peng S, Xu W, et al. Distribution and speciation of phosphorus in surface sediments of the intertidal zone in the Yellow River Delta. IOP Conference Series: Earth and Environmental Science, 2020, 621: 012091. DOI: 10.1088/1755-1315/621/1/012091.
32. Liu J, Rong Q, Zhao Y. Variations in soil nutrients and salinity caused by *tamarisk* in the coastal wetland of the Laizhou Bay, China[J]. Ecosphere, 2017a, 8(2). DOI: 10.1002/ecs2.1672.
33. Liu R, Shi W, Zhang X, et al. Effects of nitrogen starvation on *Suaeda salsa* from different habitats. Acta Ecologica Sinica, 2017b, 37(6): 1881-1887. DOI: 10.5846/stxb201511052251.
34. Liu S, Hou X, Yang M, et al. Factors driving the relationships between vegetation and soil properties in the Yellow River Delta, China[J]. Catena, 2018, 165: 279-285. DOI: 10.1016/j.catena. 2018.02. 004.
35. Liu S, Qin T, Dong B, et al. The influence of climate, soil properties and vegetation on soil nitrogen in sloping farmland[J]. Sustainability, 2021, 13(3): 1480. DOI: 10.3390/SU13031480.
36. Ma Y, Yue K, Heděnec P, et al. Global patterns of rhizosphere effects on soil carbon and nitrogen biogeochemical processes[J]. Catena, 2023, 220(PA). DOI: 10.1016/J.CATENA.2022.106661.
37. Mahbobeh I, Hossein S. Effects of soil texture and nitrogen on ability of carbon sequestration in different organs of two *Tamarix* species as a good choice for carbon stock in dry lands[J]. Ecological Engineering, 2019, 139(C): 105577. DOI: 10.1016/j.ecoleng.2019.08.007.
38. María B G, José M F, José R, et al. Strategies underlying salt tolerance in halophytes are present in *Cynara cardunculus*[J]. Plant Science, 2004, 168(3): 653-659. DOI: 10.1016/j.plantsci.2004.09.035.
39. Meysman F, Middelburg J, Heip C. Bioturbation: a fresh look at Darwin's last idea (Review). Trends in Ecology and Evolution, 2006, 21(12), 688-695. DOI: 10.1016/j.tree.2006. 08.002.
40. Meng L, Qu F, Bi X, et al. Elemental stoichiometry (C, N, P) of soil in the Yellow River Delta nature reserve: Understanding N and P status of soil in the coastal estuary. Science of the Total Environment, 2021, 751: 141737. DOI: 10.1016/j.scitotenv.2020.141737.
41. Muhammad M A, Hu X, Tariq A, et al. Carbon, nitrogen, and phosphorus stoichiometry mediate sensitivity of carbon stabilization mechanisms along with surface layers of a mollisol after long-term fertilization in Northeast China[J]. Journal of Soils and Sediments, 2020, 21: 705-723. DOI: 10.1007/s11368-020-02825-7.

42. Nakayama M, Tateno R. Solar radiation strongly influences the quantity of forest tree root exudates [J]. Trees, 2018, 32: 871-879. DOI10.1007/s00468-018-1685-0.
43. Qadir M, Ghafoor A, Murtaza G. Use of saline-sodic waters through phytoremediation of calcareous saline-sodic soils[J]. Agricultural Water Management, 2001, 50(3):197-210. DOI: 10.1016/s0378-3774(01)00101-9.
44. Qu F, Meng L, Xia J, et al. Soil phosphorus fractions and distributions in estuarine wetlands with different climax vegetation covers in the Yellow River Delta. Ecological Indicators, 2021, 125: 107497. DOI: 10.1016/J.ECOLIND.2021.107497.
45. Qu F, Meng L, Yu J, et al. Influences of micro-geomorphology on the stoichiometry of C, N and P in Chenier Island soils and plants in the Yellow River Delta, China[J]. PloS one, 2017, 12(12): e0189431. DOI: 10.1371/journal.pone.0189431.
46. Qu F, Shao H, Meng L, et al. Forms and vertical distributions of soil phosphorus in newly formed coastal wetlands in the Yellow River Delta Estuary. Land Degradation & Development, 2018, 29 (11): 4219-4226. DOI: 10.1002/ldr.3132.
47. Qu F, Yu J, Du S, et al. Influences of anthropogenic cultivation on C, N and P stoichiometry of reed-dominated coastal wetlands in the Yellow River Delta[J]. Geoderma, 2014, 235-236: 227-232. DOI: 10.1016/j.geoderma.2014.07.009.
48. Rong Q, Liu J, Cai Y, et al. “Fertile island” effects of *Tamarix chinensis Lour.* on soil N and P stoichiometry in the coastal wetland of Laizhou Bay, China[J]. Journal of Soils and Sediments, 2016, 16(3): 864-877. DOI: 10.1007/s11368-015-1296-y.
49. Sun D, Li Y, Yu J, et al. Spatial distribution of soil quality under different vegetation types in the Yellow River Delta wetland[J]. Frontiers in Ecology and Evolution, 2022b. DOI: 10.3389/FEVO.2022.977899.
50. Sun D, Yu M, Yu J, et al. Responses of soil nutrient contents and eco-stoichiometric characteristics to fiddler crab activities in coastal wetland of the yellow river delta[J]. Ecohydrology & Hydrobiology, 2022 c (3): 454-465. DOI: 10.1016/J.ECOHYD.2022.02.001.
51. Sun J, Zhao X, Fang Y, et al. Root growth and architecture of *Tamarix chinensis* in response to the groundwater level in the Yellow River Delta[J]. Marine Pollution Bulletin, 2022a, 179: 113717. DOI: 10.1016/j.marpolbul.2022.113717.
52. Sun L, Ataka M, Kominami Y, et al. A constant microbial C/N ratio mediates the microbial nitrogen mineralization induced by root exudation among four co-existing canopy species[J]. Rhizosphere, 2021, 17: 100317. DOI: 10.1016/J.RHISPH.2021.100317.
53. Tian P, Chen C, Zhao H, et al. Enzyme activities and microbial communities in rhizospheres of plants in salinized soil in North Yinchuan, China. Acta Pedol. Sin, 2020, 57(1), 217-226. DOI 10.11766/trxb201807050359.
54. Wang Z, Zhu S, Yu R, et al. Saline Soil in China. Beijing: Science Press, 1993: 36-346. 7030037944.
55. Wang D, Bai J, Zhao Q, et al. Profile differentiation of soil salinity for natural and anthropogenic disturbance wetlands in the Yellow River Delta[J]. J Journal of Natural Resources, 2020, 35(2): 438-

448. DOI: 10.31497/zrzyxb.20200215.

56. Wang R, Cavagnaro T R., Jiang Y, et al. Carbon allocation to the rhizosphere is affected by drought and nitrogen addition[J]. Journal of Ecology, 2021, 109(10): 3699-3709. DOI: 10.1111/1365-2745.13746.
57. Wang W, Sardans J, Wang C, et al. The response of stocks of C, N, and P to plant invasion in the coastal wetlands of China[J]. Global Change Biology, 2019, 25(2): 733-743. DOI: 10.1111/gcb.14491.
58. Wendel A S., Bauke S L., Amelung W, et al. Root-rhizosphere-soil interactions in biopores[J]. Plant and Soil, 2022, 475(1-2): 253-277. DOI: 10.1007/S11104-022-05406-4.
59. Wu X, Bi N, Xu J, et al. Stepwise morphological evolution of the active Yellow River (Huanghe) delta lobe (1976-2013): Dominant roles of riverine discharge and sediment grain size[J]. Geomorphology, 2017, 292: 115-127. DOI: 10.1016/j.geomorph.2017.04.042.
60. Xiong J, Shao X, Yuan H, et al. Carbon, nitrogen, and phosphorus stoichiometry and plant growth strategy as related to land-use in Hangzhou Bay Coastal Wetland, China[J]. Frontiers in Plant Science, 2022, 13: 946949. DOI: 10.3389/FPLS.2022.946949.
61. Xu C, Pu L, Li J, et al. Effect of reclamation on C, N, and P stoichiometry in soil and soil aggregates of a coastal wetland in eastern China[J]. Journal of Soils and Sediments, 2019, 19(3): 1215-1225. DOI: 10.1007/s11368-018-2131-z.
62. Yamamoto K, Shiwa Y, Ishige T, et al. Bacterial diversity associated with the rhizosphere and endosphere of two halophytes: *Glaux maritima* and *Salicornia europaea*[J]. Frontiers in microbiology, 2018, 9: 2878. DOI: 10.3389/fmicb.2018.02878.
63. Yang C, Chen H, Li J, et al. Soil improving effect of *Suaeda salsa* on heavy coastal saline-alkaline land[J]. Chinese Journal of Eco-Agriculture, 2019, 27(10): 1578-1586. DOI: 10.13930/j.cnki.cjea.190178.
64. Ye J, Perez P G, Zhang R, et al. Effects of different C/N ratios on bacterial compositions and processes in an organically managed soil[J]. Biology and fertility of soils: Cooperating Journal of the International Society of Soil Science, 2018, 54(1): 137-147. DOI: 10.1007/s00374-017-1246-5.
65. Yi L, Ma J, Li Y. Soil salt and nutrient concentration in the rhizosphere of desert halophytes[J]. Acta Ecologica Sinica, 2007a, 27(9): 3565-3571. DOI: 10.1016/S1872-2032(07)60074-2.
66. Yi L, Ma J, Li Y. Impact of salt stress on the features and activities of root system for three desert halophyte species in their seedling stage[J]. Science China Earth Sciences, 2007b, 50(Suppl 1): 97-106. DOI: 10.1007/s11430-007-5012-7.
67. Yu J, Zhan C, Li Y, et al. Distribution of carbon, nitrogen and phosphorus in coastal wetland soil related land use in the Modern Yellow River Delta[J]. Scientific reports, 2016, 6(1): 37940. DOI: 10.1038/srep37940.
68. Yuan Z, Druzhinina I S, Labbé J, et al. Specialized microbiome of a halophyte and its role in helping non-host plants to withstand salinity[J]. Scientific Reports, 2016, 6(1): 32467. DOI: 10.1038/srep32467.

69. Zhang J, Shi H. Physiological and molecular mechanisms of plant salt tolerance[J]. Photosynthesis research, 2013, 115(1): 1-22. DOI: 10.1007/s11120-013-9813-6.
70. Zhang Q, Wang Z, Xia S, et al. Hydrologic-induced concentrated soil nutrients and improved plant growth increased carbon storage in a floodplain wetland over wet-dry alternating zones[J]. Science of the Total Environment, 2022, 822: 153512. DOI: 10.1016/J.SCITOTENV.2022.153512.
71. Zhang Z, Lu X, Song X, et al. Soil C, N and P stoichiometry of *Deyeuxia angustifolia* and *Carex lasiocarpa* wetlands in Sanjiang Plain, Northeast China. Journal of Soils & Sediments: Protection, Risk Assessment, & Remediation, 2012, 12 (9), 1309-1315. DOI: 10.1007/s11368-012-0551-8.
72. Zhao X, Tian P, Sun Z, et al. Rhizosphere effects on soil organic carbon processes in terrestrial ecosystems: A meta-analysis[J]. Geoderma, 2022a, 412: 115739. DOI: 10.1016/J.GEODERMA.2022.115739.
73. Zhao Y, Li T, Liu J, et al. Ecological stoichiometry, salt ions and homeostasis characteristics of different types of halophytes and soils[J]. Frontiers in Plant Science, 2022b, 13: 990246. DOI: 10.3389/FPLS.2022.990246.
74. Zhao Y, Li T, Shao P, et al. Variation in bacterial community structure in rhizosphere and bulk soils of different halophytes in the Yellow River Delta. Frontiers in Ecology and Evolution, 2022c, 9: 816918. DOI: 10.3389/FEVO.2021.816918.
75. Zheng Y, Hou L, Chen F, et al. Denitrifying anaerobic methane oxidation in intertidal marsh soils: Occurrence and environmental significance[J]. Geoderma, 2020, 357(C): 113943. DOI: 10.1016/j.geoderma.2019.113943.
76. Zhu X. Pedology (Volume ii). Beijing: Agricultural Press, 1983: 347-359. 80407042.

Figures

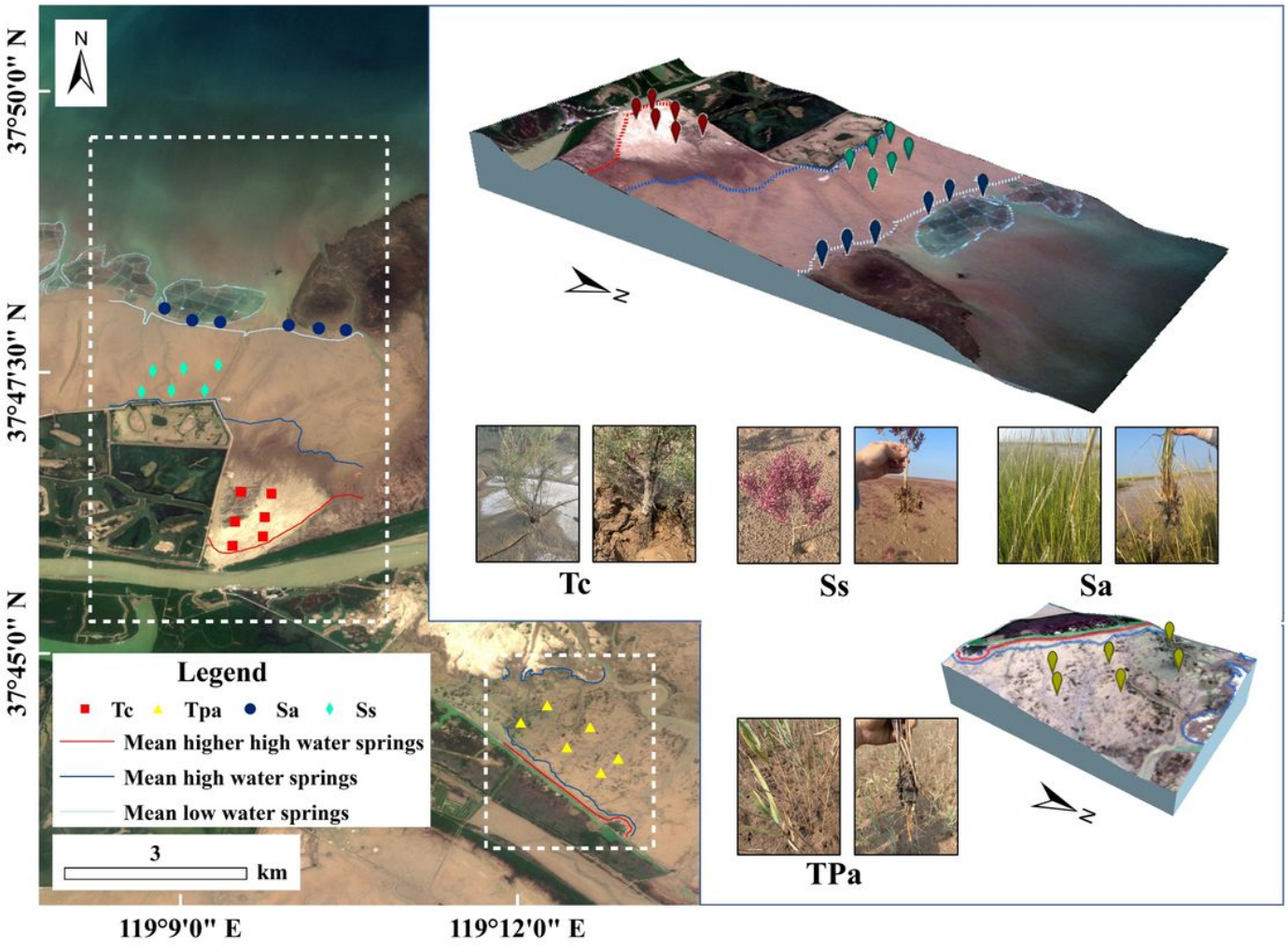


Figure 1

Study area and sample sites of *Tamarix chinensis* (Tc), *Phragmites australis* (tidal salt community, TPa), *Suaeda salsa*(Ss) and *Spartina alterniflora* (Sa) in the Yellow River Estuary.

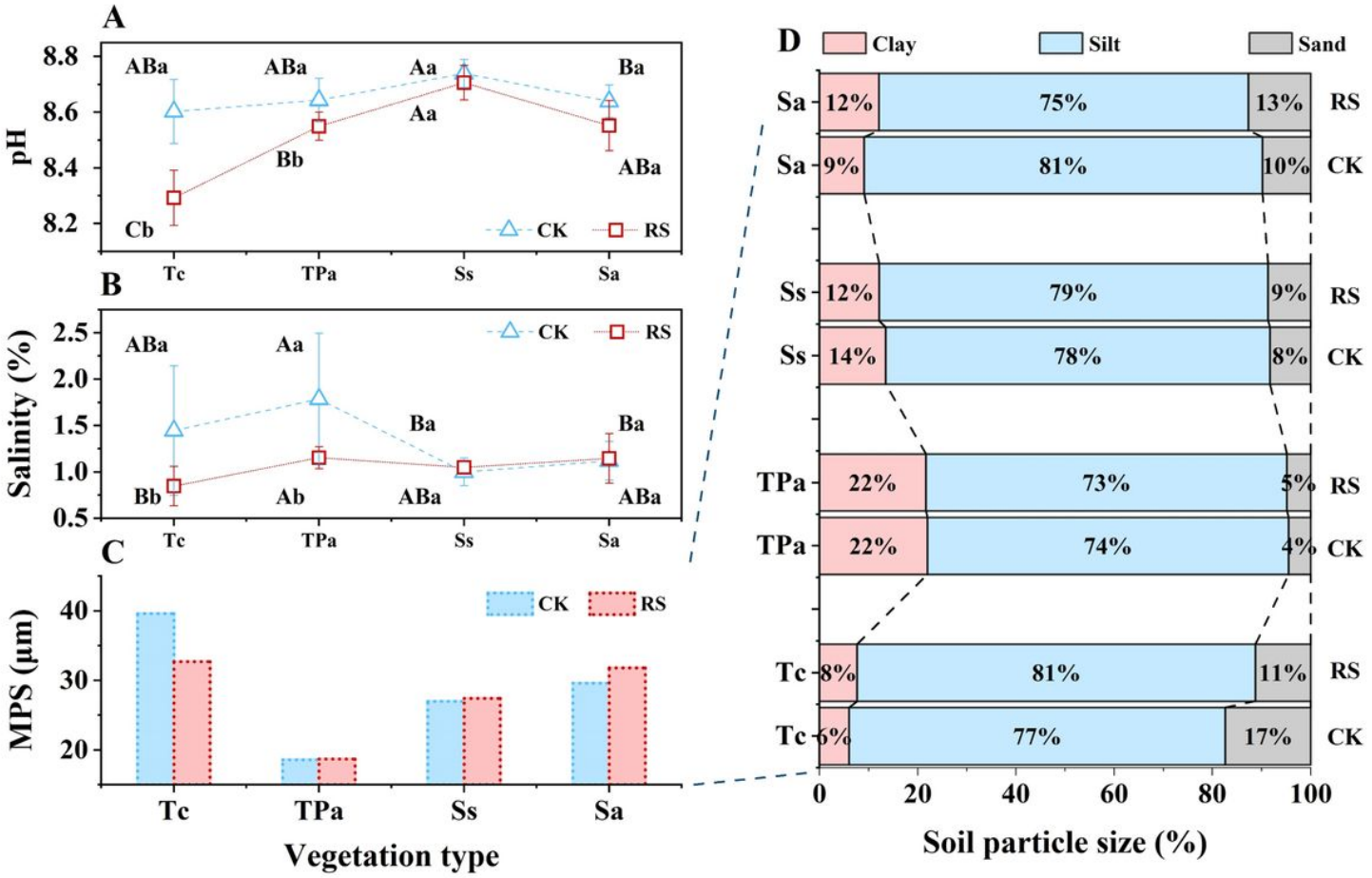


Figure 2

The soil pH (A), salinity (B) and mean soil particle size (C-D) in different halophyte types. The vertical bar is standard deviation; different lower letter denotes the significant differences among soil types for the same halophyte type ($p < 0.05$); different upper letter denotes the significant differences among halophyte types for the same soil type ($p < 0.05$).

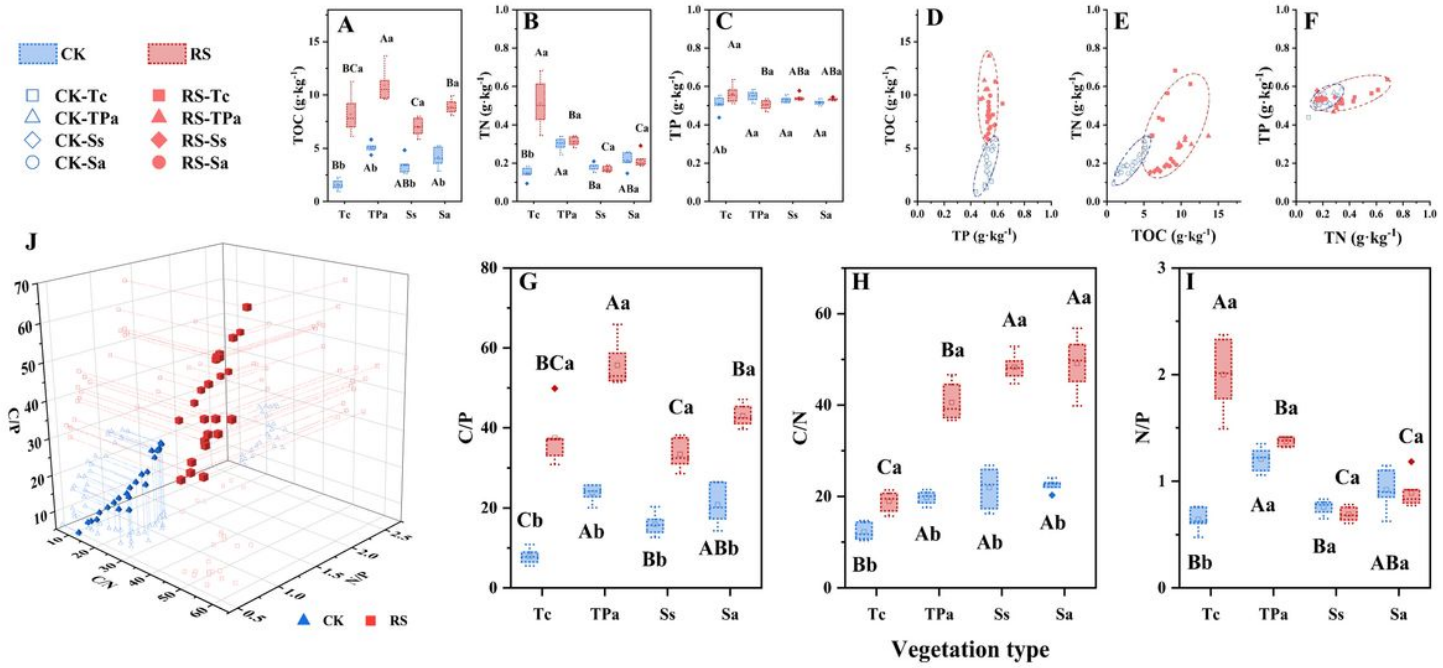


Figure 3

The contents of soil TOC (A), TN (B), TP (C), confidence distribution of C, N, and P (D-F) and ecological stoichiometry of C, N, and P (G-J) in different halophyte types. The vertical bar is standard deviation; different lower letter denotes the significant differences among soil types for the same halophyte type (p< 0.05); different upper letter denotes the significant differences among halophyte types for the same soil type (p < 0.05).

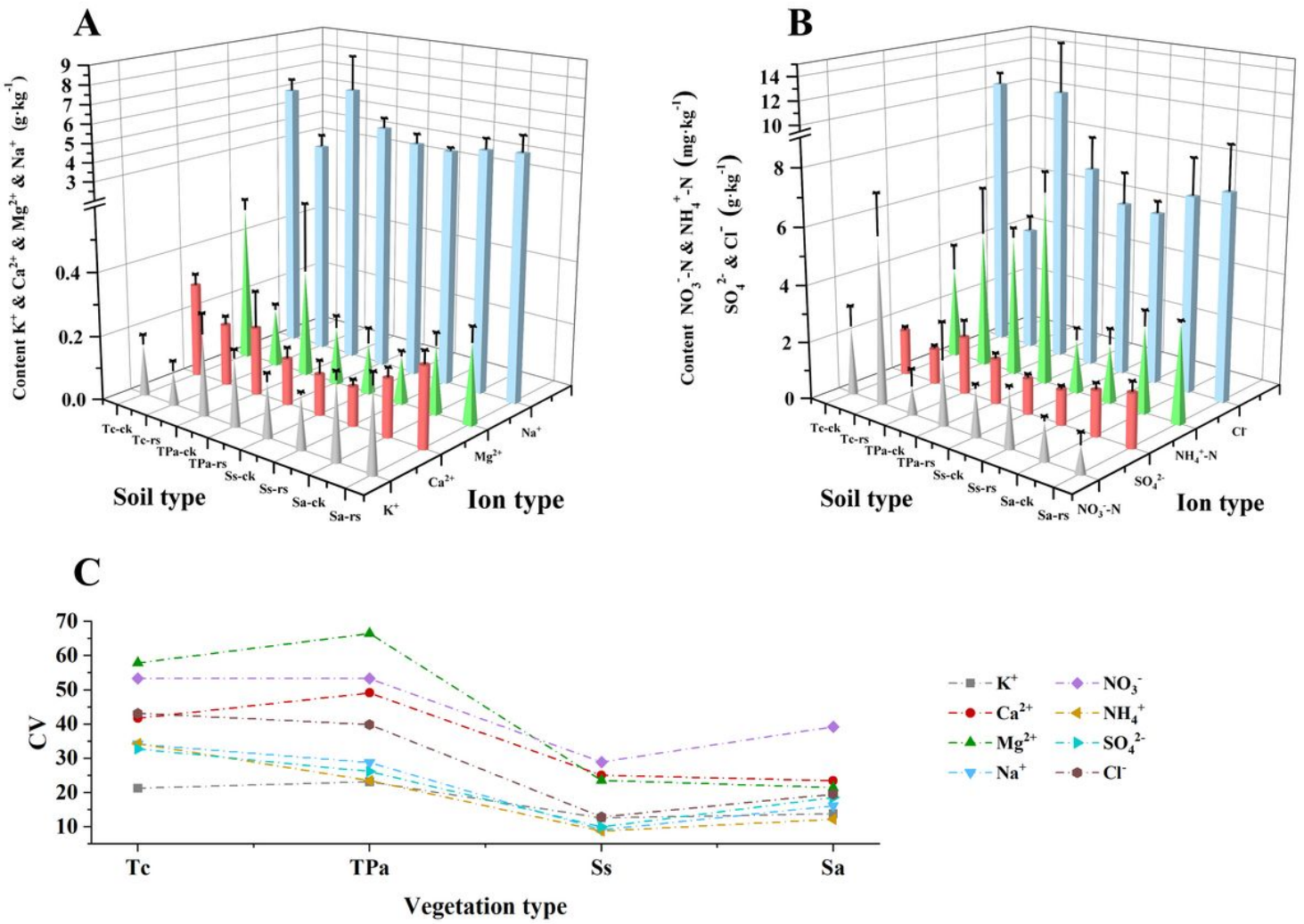


Figure 4

The soil ion contents (A-B) and their coefficient of variation (C) in different halophyte types (rs: RS group, ck: CK group).

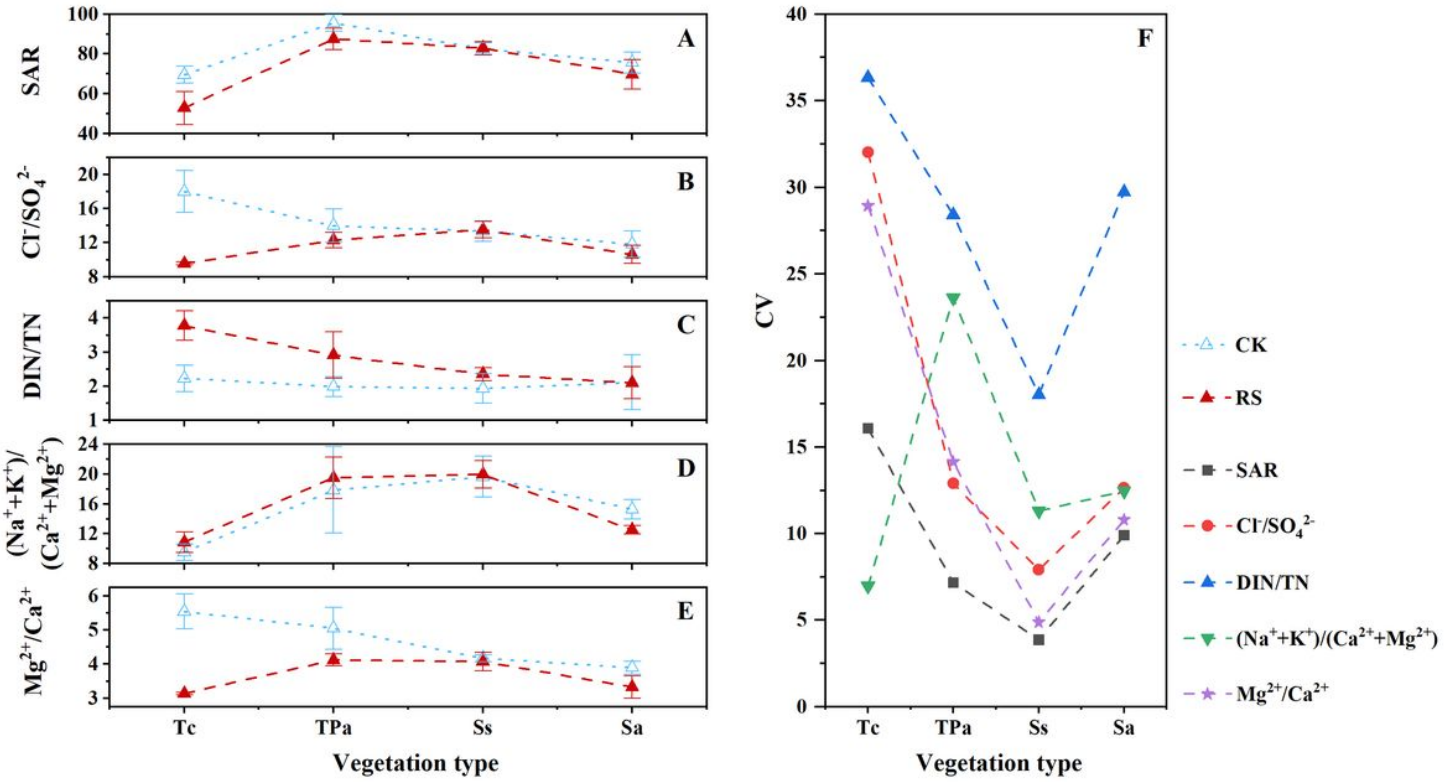


Figure 5

The soil sodium-adsorption ratio (SAR), DIN/TN, salt ions stoichiometry (A-E) and their coefficient of variation (F) values in different halophyte types.

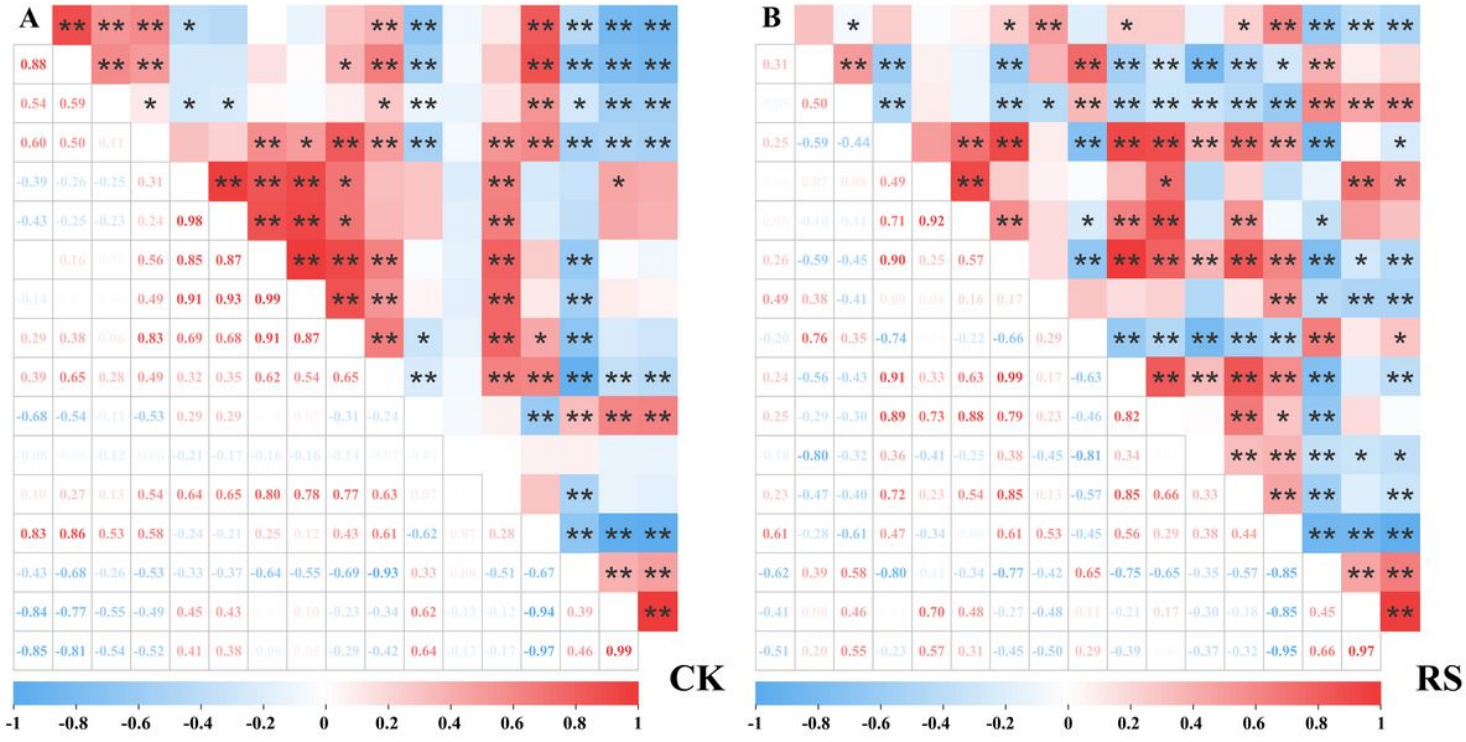


Figure 6

Pearson's correlation of soil properties of CK group (A) and RS group (B). The * denotes the $p < 0.05$, and the ** denotes the $p < 0.01$.

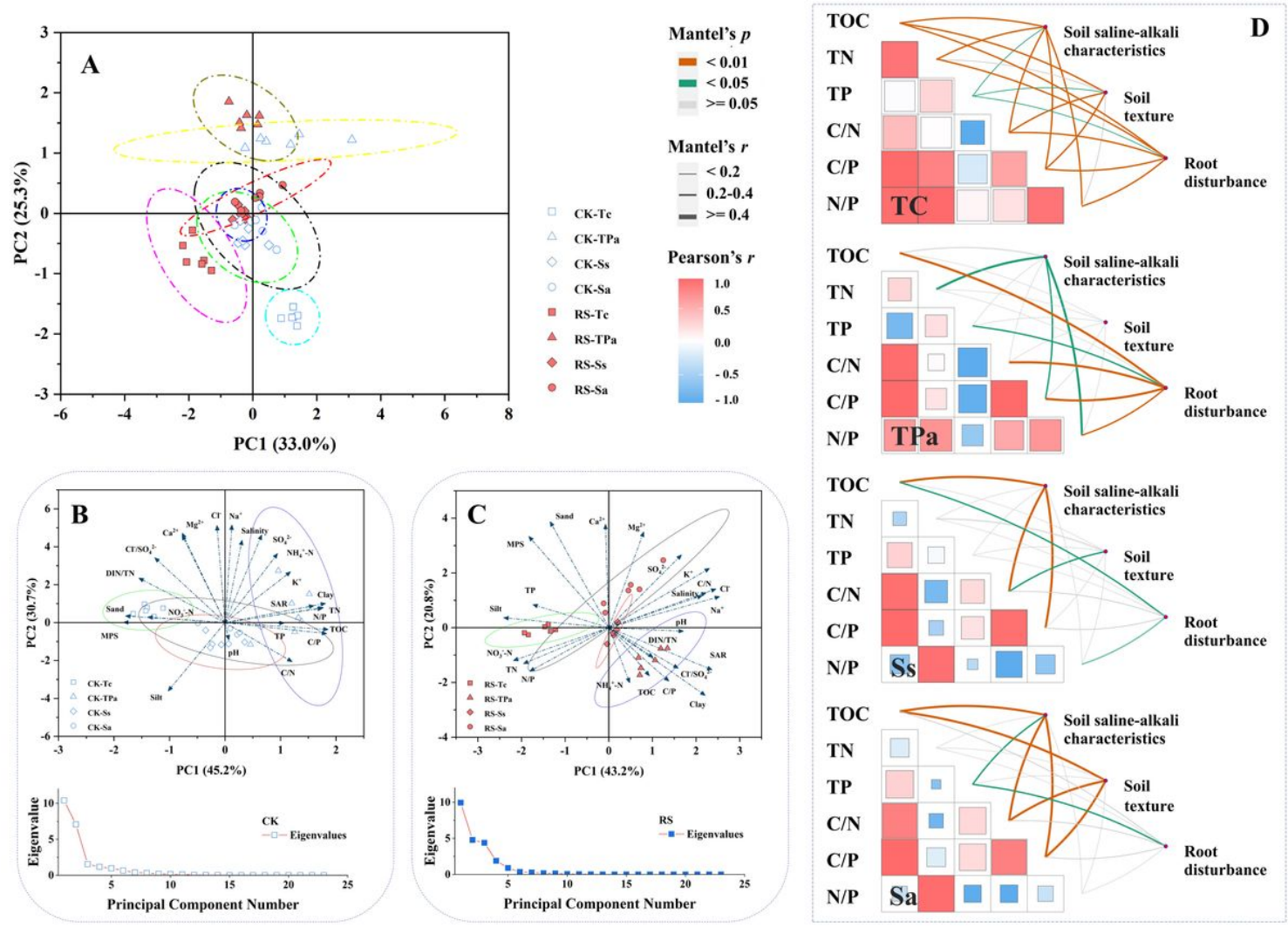


Figure 7

The PCA of soil properties (A) in CK group (B) and RS group (C), respectively, and the mantel test results of soil C, N, and P in each vegetation types (D).